CONCRETE RESEARCH LETTERS

www.crl.issres.net Vol. 7 (1) – March 2016

Structural Behavior of Light Weight Ferrocement Columns

Yousry B. I. Shaheen[1], Zeinab A. Etman[1,c] and Ahmed G. Ramadan[2]

[1]*Department of Civil Engineering, Faculty of Engineering, Menoufia University, EGYPT.*
[2] *Civil Engineer and Postgraduate Fellow*

Received: 30/11/2015 – Revised: 15/03/2016 – Accepted: 28/03/2016

Abstract

This paper presents the results of the behavior of reinforced ferrocement lightweight columns by permanent precast lightweight ferrocement hollow blocks. For this objective, an experimental program was carried out extensively and finite element models with ANSYS 14.5 were conducted. The program of the experimental constructed and testing of sixteen columns of total dimensions 450×650×250 mm consisting of 3 permanent precast lightweight ferrocement hollow blocks having the dimensions of 200×400×200 mm filled with core material. Two types of light weight ferrocemnet hollow blocks were used to construct the columns. Two types of single layer welded steel mesh and glass fiber mesh were used as a horizontal connection between the permanent precast lightweight ferrocement hollow blocks. The core material was investigated: one layer of welded steel mesh embedded in the matrix. Welded steel mesh with single and double layers was used to reinforce the plastering layer as a bonding layers forms; namely welded steel mesh. Shear connections between the permanent precast hollow blocks and the core material were investigated called; shear connector. The columns were tested under uniform load. The behavior of the columns was compared. The results showed that an improvement in the cracks resistance, serviceability loads, ultimate loads, and energy absorption. These results were verifies the validity of the proposed model. Good agreement was found compared with the experimental results. Out of this research, this paper presents applications of using light weight ferrocement units in construction of low-cost housing which are very useful for developed and developing countries alike with great economic advantages.

Key word: ferrocement, columns, steel mesh, light weight, ANSYS

1. Introduction

Ferrocement is a type of thin wall reinforced concrete construction where hydraulic cement is reinforced with layers of continuous and relatively small diameter mesh (Wang, S., et al. 2004 , Gaba, H., and Singh H., 2008, Naaman A. E., 2000, Wafa, M.a., and Fukuzawa K., 2010, Eltehawy, E.,(2009). The basic parameters which characterize ferrocement are the volume fraction and specific surface area of the steel meshes and the surface cover of the mortar over the steel meshes. Ferrocement is the first invention of reinforced concrete (Jagannathan, A. 2005). The behavior of ferrocement like reinforced concrete with the essential difference being that crack development is retarded by the dispersion of the reinforcement in fine form through the mortar.

[c] corresponding Author: Zeinab A. Etman,
E-mail: zeinab.etman@sh-eng.menofia.edu.eg; Telephone: +201009727355

Due to the characteristics/mechanical properties of ferrocement more applications such as: environmentally friendly, sound technology; tensile strength (Greepala and Nimityongskul, (2008), Sasiekalaa K. and Malathy R., November 2012), improved toughness, fire resistance, water tightness, resistance to cracking, lightness, durability, cost, time and construction technology cannot be matched by another thin construction material (Sasiekalaa K. and Malathy R., November 2012 , ACI Committee 549 1R-97 (1997). Brick construction for multistory buildings was very largely displaced by steel and reinforced concrete-framed structures, although these were very often clad in brick, [10].

In earthquake prone areas, the development of an effective level of bonding between mortar and bricks is essential to resist shear cracking. Bricks might be had specially shaped to create mechanical interlocking and improve bonding. Brick construction is relatively cheap and simple. In certain cases bricklaying may require skilled labor; however, this type of construction is usually performed as self-built construction, (D'Ayala D). On the other sides, the performance of masonry depends on the brick units and the mortar and their composite behavior. Guidelines were provided by building codes to optimize the strength and the performance of the structural members made of these components, (D'Ayala D).

The lightweight hollow blocks are mainly driven by the cost reduction resulting from the many materials such as the reduced dead load, the smaller sections, which require less reinforcement and the ease in construction, (ACI Committee 213R-87, 1999). The behavior of precast U -shaped ferrocement laminates was analyzed by Tawab, A. A et al., (2012). Fahmy E. H. et al., (March 2014) presented the results of experimental and theoretical study of the behavior of reinforced concrete beams consisting of precast permanent U-shaped. Mustapha M.L. and Salihuddin R.S, (2013) have reported a review on cold-formed-ferrocement composites. The results showed that the cold-formed-ferrocement composites were promising and possess good; ultimate capacity, reduced crack width, flexural and impact strengths, retrofitting capability, fire resistance, energy absorption, ductility, insulation resistance, pull-out resistance, shear resistance etc. Moreover, composites specimens have the capability and high tendency of improving performances of structures to be constructed compositely and will improve corrosion prevention etc.. An experimental results on the tensile strength of ferrocement with respect to specific surface were presented by Bhalsing S. et al. (2014).

The results showed that; the increase in tension due to increase in contact area between mortar and steel wire meshes, i.e. increase in specific surface of ferrocement. The behavior of wall panels using the technology of ferrocement was presented by Grija S. et al., (2014). The experimental and theoretical investigation was carried out when the specimens subjected to axial load. Fahmy et al. (2005) have studied the behavior of wall panel under axial load and flexural load by developing a three dimensional finite element models. They reported that the developed finite element model accommodates the non-linear material properties of the components of the Ferrocement panel due to yielding of the reinforcement, cracking of the ferrocement mortar and crushing of the ferrocement mortar. Al-Rifaie W.N. and Jomaah M.M. (2010) have presented an investigation of two ferrocement channel-like beams to form I-cross section beam and four ferrocement plates are cast and tested due to bending loading.

The structural behavior was recorded by reading the deflection and by observing the crack patterns. The recorded values of deflections and the observations indicated that ferrocement can be used in construction of buildings (Al-Rifaie W.N. and Jomaah M.M. (2010).

2. Research significance

This paper was carried out to investigation the structural behavior of ferrocement masonry light weight columns. The column was constructed with permanent precast lightweight ferrocement hollow block. This paper presents an application of using permanent precast light

weight ferrocement hollow block in construction the masonry columns as an applications of using the ferrocement technology in the light weight units and low-cost housing. The effect of core material, types and numbers of layers used with plastering layers was also investigated.

3. Experimental Program

The experimental work consisted of sixteen columns of total dimensions 450×650×250 mm, which consists of 3 permanent precast lightweight ferrocement hollow blocks having the dimensions of 200×400×200 mm filled with core material and without core materials. Two types of the permanent precast units used in construction of columns forms; lightweight ferrocement hollow block reinforced with one layer of welded steel meshes and lightweight ferrocement hollow block reinforced with one layer of glass fiber meshes.

Table 1 and Figure 1 show the details of the experimental program. The symbols were used for the sample code: the first letter realizes the type of mesh (W: welded steel mesh and G: glass fiber mesh), the second letter realizes the core maters (M: the columns without reinforcement for the core material, and R: the column with reinforcement for core material), the third letter realizes the numbers of reinforcing mesh layers (O: no layer, S: single layer and D: double layers), the fourth letter realizes the shear connection (C: shear connection). The tested columns were divided into four groups.

Group number 1 (GM): in this group the construction of columns was using permanent precast light weight ferrocement hollow block reinforced with glass fiber mesh. One layer glass fiber mesh was used to reinforce the horizontal connection for this group. The hollow cores of this group were filled with mortars only. Group number 2 (GR): in this group the construction of columns was using permanent precast light weight ferrocement hollow block reinforced with glass fiber mesh. One layer glass fiber mesh was used to reinforce the horizontal connection for this group. Therefore, in this group the hollow cores were filled with mortars reinforced with one layer of welded steel mesh.

Group number 3 (WM): in this group the columns constructs using permanent precast light weight Ferrocement hollow block reinforced with welded steel mesh. One layer welded steel mesh was used to reinforce the horizontal connection for this group. The hollows of this group were filled with mortar only. Group number 4 (WR): in this group the construction of columns was using permanent precast light weight ferrocement hollow block was reinforced with welded steel mesh. One layer welded steel mesh was used to reinforce the horizontal connection for this group. In this group the hollows were filled with mortars reinforced with one layer of welded steel mesh.

The details of light weight ferrocement hollow block units were reported by Shaheen et al., 2014. Single and double layers steel meshes were used to reinforce the plastering as a bonding layer forms; namely welded steel meshes. Shear connections were used to connect the permanent hollow blocks and the core mortar were namely; mechanical shear connectors. Shear connection were used to connect the two surfaces and the core materials was carried out by fixing bolts through fisher's insides of the forms.

3.1. Materials properties

Ordinary Portland cement type (CEMI 42.5N) according to the requirements of E.S.S.4756-11, 2007 with a specific gravity of 3.16 and a specific surface area (Blaine fineness) 3740 cm²/gm was used. Locally produced identified silica fume (S.F.) was delivered in 25-Kg sacks according to the manufacturer; the powder had an average particle size of 0.1 micrometer, specific surface area 170000 cm^2/gm and specific gravity of 2.2. Natural siliceous sand was used as fine aggregates throughout the current research.

The fine aggregates used was obtained from Suez zone with 2.6 specific gravity and 3.28 fineness modulus and the percentage of particles finer than sieve No. 200 resulted absorption percentage of 0.81%. High range water reducer (HRWR) of a synthetic type dispersion base was used to improve the mixes workability. HRWR complies with ASTM C494 (2001) Type A & F and B.S. 5075 Part 3(June 2009).

Galvanized welded steel wire mesh of 0.8 mm in diameter and size of openings 12.7 x 12.7 mm in spacing was used for reinforcing the core and the plastering layer as showed in Figure 2. Glass fibers meshes with weight 90 gm/m^2, and size of openings 11.5 x12.5 mm in spacing was used for horizontal connection as showed in Figure 2. The proof stress and the tensile strength were 485 and 560 MPa, respectively for steel wire mesh as tensile tests resulted. Tensile tests on glass fiber mesh showed that the tensile strength and elongations were 155 MPa and 4.5%, respectively.

These values comply with of ACI 549.1R-97 (1997). Steel bolts of 50 mm length and 6 mm diameter were used for shear connection. The proof stress and ultimate strength of steel bolts were 400MPa and 510 MPa, respectively.

TABLE 1: SCHEME OF THE EXPERIMENTAL PROGRAM.

Code		Steel meshes				Core materials	Dimensions of Specimen (mm)
		type	No. of layers	V_f (%)	Total weight of steel (kg)		
Group GM	GMO	Glass fiber mesh	-	-	0.5	Mortar	450 × 650 × 250
	GMS		1	1.64	0.67		
	GMD		2	2.63	0.84		
	GMSC		1	1.64	0.94		
Group GR	GRO		-	-	0.6	Mortar reinforced with welded steel mesh	
	GRS		1	1.64	0.77		
	GRD		2	2.63	0.95		
	GRSC		1	1.64	1.05		
Group WM	WMO	Welded steel mesh	-	-	0.6	Mortar	
	WMS		1	1.64	0.77		
	WMD		2	2.63	0.95		
	WMSC		1	1.64	1.05		
Group WR	WRO		-	-	0.8	Mortar reinforced with welded steel mesh	
	WRS		1	1.64	0.97		
	WRD		2	2.63	1.15		
	WRSC		1	1.64	1.25		

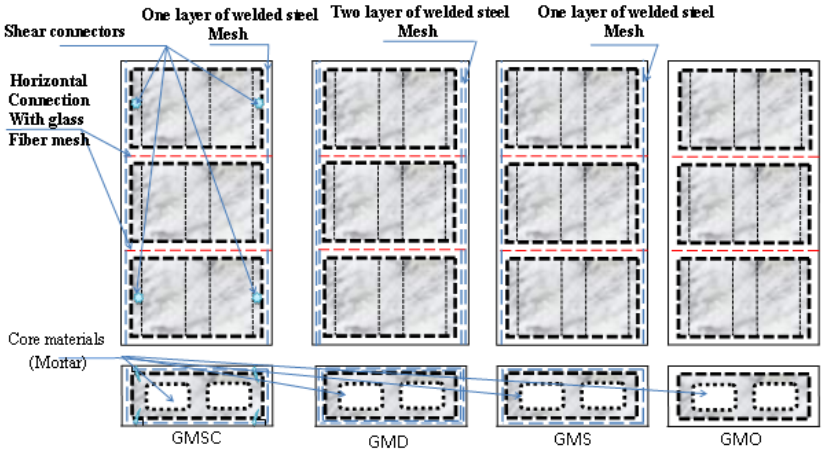

Group (GM) specimens.

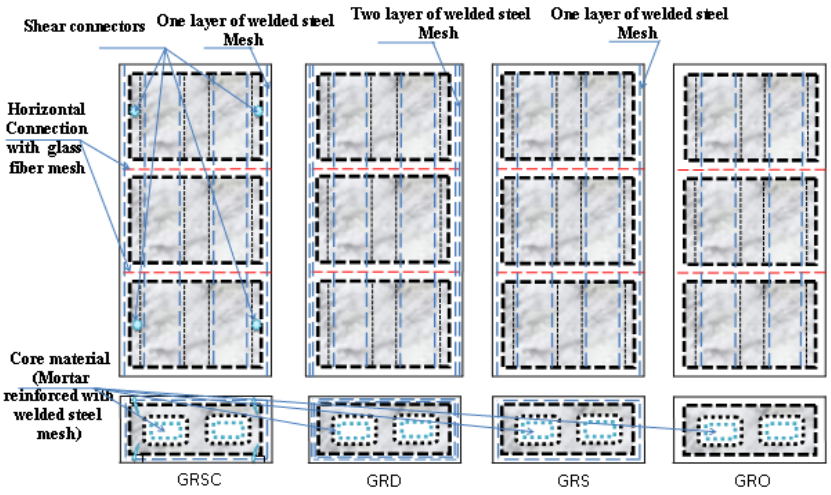

Group (GR) specimens.

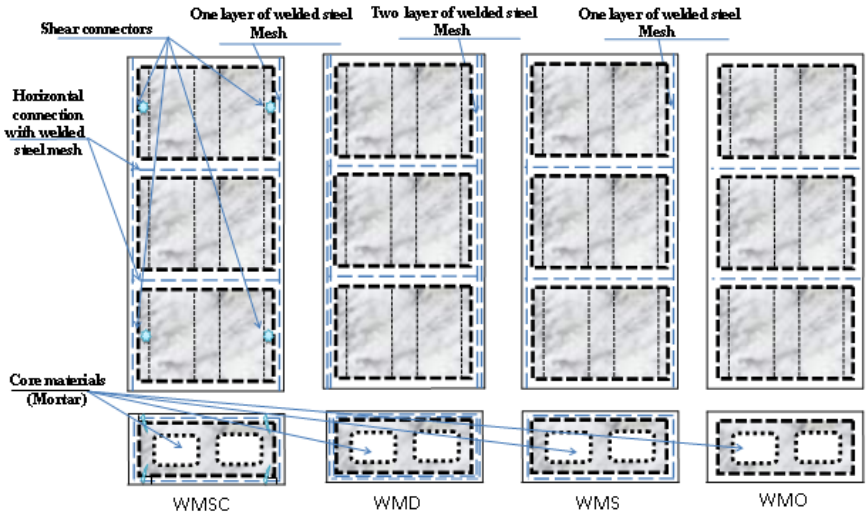

Group (WM) specimens.

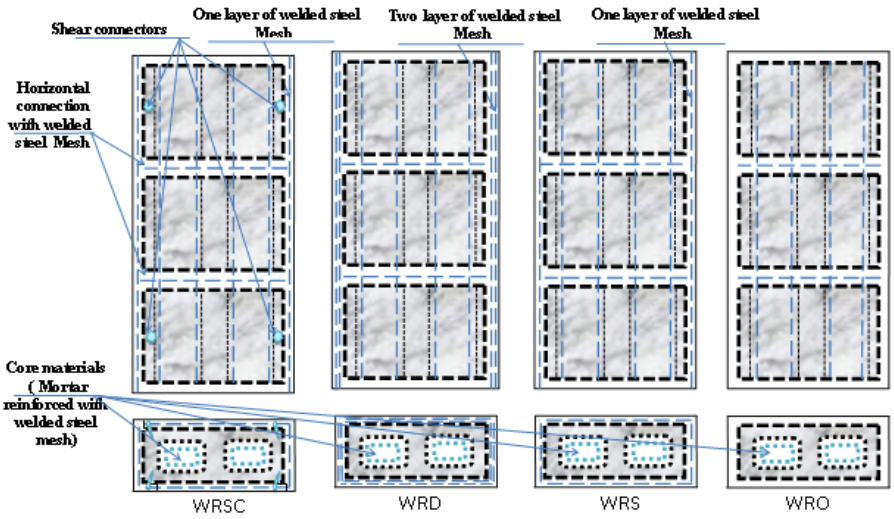

Group (WR) specimens.

Figure 1: Details of Bonding Arrangement for Reinforced Masonry Columns Units.

3.2. Preparation of masonry columns

Figure 3-a shows the mold of the hollow block unit. The mold was manufactured to cast the lightweight ferrocement hollow blocks having the dimensions of 200×400×200 mm. The steel wire mesh was formed. The mortar were mixed and cast in the mold as shown in Figure 3. The blocks were left for 24 hr. in the mold. These forms were cured for 28 days and then were stored.

The mix was used for cast these forms were illustrated in Table 2. The compressive strength of the ferrocement hollow blocks was 7.6 MPa with weights 10.8 kg which put them at the load bearing category according to ASTM C90 – 11, (2011), ASTM C129 – 06, (2007), IBC (2012) and E.S.S. 2005/429 (2005).The preparing hollow blocks were used as permanent forms to construct the masonry columns. Sand, ordinary Portland cement and lime as a sand-cement mortar were used for plastering. The mortars used for building, plastering and the core was cement lime mortar as shown in Table 3 which conforming to requirements of ASTM C270-7(2007). Polypropylene fibers (fiber mesh 300-e3) were added by 1200 gm/m³. 50×50×50 mm cube was used to determine the compressive strength of the mix.

After 28 days, the compressive strength was obtained by testing three cubes for the mix. Columns specimens were constructed of 6 permanent precast light weight ferrocement hollow blocks of total dimensions of 450×650×250 mm and filled with the core materials. During construction works the columns samples; horizontal reinforcement with one layer of welded steel mesh or glass fiber mesh between blocks were applied. Also, vertical reinforcement with one, two and three layers of welded steel mesh over the columns units was applied. The core material was cast to fill the holes of the columns.

Figures 4 to 10 show the steps of masonry columns. In Figure 9; steel wire meshes were formed into cages of dimensions 220×420×600 mm and enwrapped around specimens to apply plastering. After that shear connectors between the two surfaces and the core materials was carried out by fixing bolts through the sides of the specimens. Also plastering works executed by mortar (SP), Figure 10. After finishing all columns specimens were cured by damp canvas till tested.

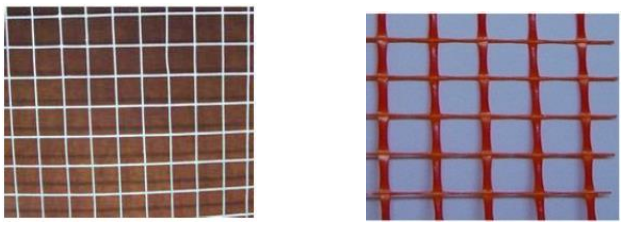

Figure 2: Galvanized welded wire steel mesh and Fiber glass mesh.

a) The mold b) Forming the steel mesh c) Cast the hollow block

d) Ferrocement hollow block

Figure 3: Procedures of manufactured hollow blocks units.

Table 2: Mix Proportions of Permanent Precast Light Weight Ferrocement Hollow Blocks (kg/m^3).

Cement	Sand	Water	Super plasticizer	Silica Fume	EPS	Cube Compressive Strength(MPa)			Average dry Density (Kg/m ^{3})
						7days	28days	3months	
428	1015	211	9.4	42	9.4	**7.66**	**9.66**	**15.33**	**1719.44**

Table 3: Mortar Proportion According to ASTM C270.

designation code	Portland Cement	Lime	Sand	water	Polypropylene fiber gm/m^3	Min 28-days Compressive Strength, MPa
SP	1	0.5	4.5	75	`1200	1800

Figure 4: Steps of Masonry Construction for Columns Specimens.

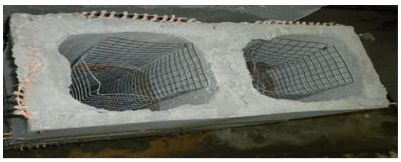

Figure 5: Steel wire mesh box reinforcement arrangement inside the holes of column specimens.

Figure 6: Column specimens after filling the holes by mortar (SP).

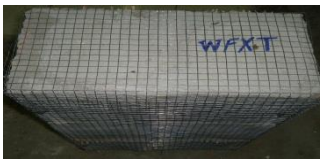

Figure 7: Steel wire meshes after formed into cages and enwrapped around walls specimens.

Figure 8: Mechanical shear connectors.

Figure 9: Drilling the holes for the connectors.

Figure 10: Column specimen after apply plastering works by mortar (SP).

4. Test set-up

Figure 11 shows the sketch of the test set-up. During the testing to clarify the visual cracks white paint was used. To measure the strain, a group of demec points was placed during loading. Five dial gauges were positioned to measure the displacements during the loadings. A steel plate with 30mm thickness was used at the top surface of the tested column for producing uniform distributed loadings in testing the performance of the masonry wall units.

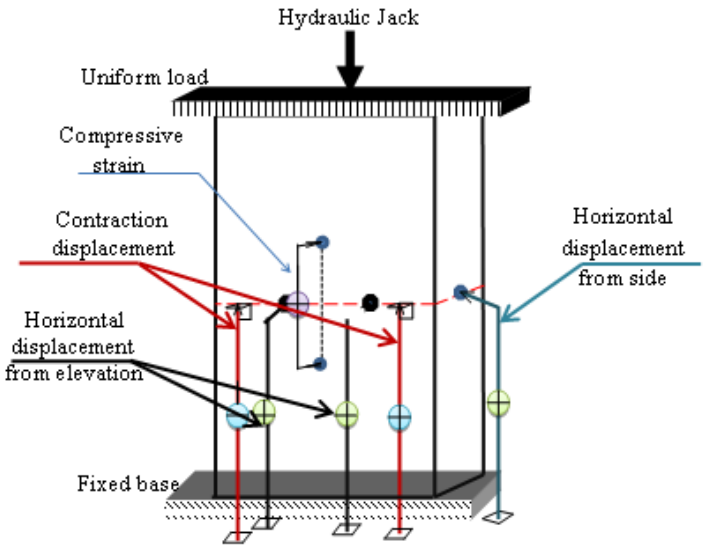

Figure 11: Test set-up and Locations of the demec points.

5. Discussions of test results of masonry columns

The column specimens were tested under uniformly compression loadings up to failure and the cracking. During the test; visual detects with recording contractions displacement and horizontal displacement of columns specimens' sides and elevations. Table 4 shows the test results of the tested masonry columns such as horizontal and contraction displacements performance in terms of compressive strength, compressive strain, initial cracking and ultimate load. The load-horizontal displacements and the load-strain for the test specimens were illustrated in Figures 12 to 15. Serviceability load and the energy absorptions for the masonry walls were illustrated in Table 4. Egyptian code (2007) defines the serviceability load as the load corresponding to a deflection equal to height/180 which is allowed deflection. The area under the load-deflection curve is defined as the energy absorption.

The masonry wall filled with mortar achieved better results compared to that of the control specimen. The percentage of increase in the mechanical properties of the masonry walls changed with the number of steel meshes of the plastering layer and the core materials. The mechanical properties of horizontal displacement, first crack, serviceability load, ultimate load, modes of failure, and energy absorption are resulted.

5.1. Effect of type of permanent precast lightweight ferrcement hollow blocks.

Two types of permanent precast lightweight ferrocement hollow blocks were used to construct the columns. One type of the permanent hollow block reinforced with one layer of welded steel meshes and the other reinforced with one layer of glass fiber meshes.

From Table 4, the results clear that the first crack for the unites reinforced with glass fibers was noticed at 200 kN while it was noticed at 150 kN for the unites reinforced for welded steel mesh. The opposite was occurred at the ultimate load. The ultimate load for the columns constructed with the hollow block reinforced with welded steel meshes was higher that the ultimate load for the columns constructed with the hollow block reinforced with glass fiber meshes by 33%. Also the ductility index, the serviceability load and energy absorption were higher for the columns constructed with the hollow block reinforced with welded steel fiber meshes than that the ultimate load for the columns constructed with the hollow block reinforced with glass fiber meshes by 160%, 36% and 65% respectively.

Table 4: test results for the masonry columns.

Code		First crack load (kN)	Ultimate load (kN)	Serviceability load (kN)	Horizontal displacement at				Ductility index	Energy absorption (kN.mm)
					first cracks (mm)		ultimate load (mm)			
					Side	elevation	Side	elevation		
Group GM	GMO	200	450	310	0.62	1.05	3.00	2.8	3.7	907.5
	GMS	200	600	415	0.45	0.70	2.20	8.2	8.3	1360
	GMD	250	650	450	0.11	1.45	1.30	8.5	8.84	1499
	GMSC	250	500	335	0.62	1.2	1.30	3.7	3.08	950
Group GR	GRO	200	500	345	0.55	1.0	2.00	4.3	3.97	1293
	GRS	200	600	415	0.75	0.66	5.00	5.0	7.12	1500
	GRD	200	600	420	0.73	0.65	2.55	3.2	4.9	1530
	GRSC	100	450	315	0.61	1.74	3.61	7.5	5.9	1500
Group WM	WMO	150	600	422	0.65	0.45	5.00	5.22	7.69	1500
	WMS	150	600	425	0.65	0.5	4.80	3.2	7.38	1540
	WMD	200	650	446	0.79	0.55	2.00	4.3	7.81	1597.5
	WMSC	150	650	442	0.38	0.33	2.30	3.2	9.69	1548
Group WR	WRO	100	550	374	0.6	0.40	4.80	3.1	8	1320
	WRS	150	650	445	0.85	0.90	4.75	3.7	5.58	1425
	WRD	100	700	476	0.2	1.44	2.70	5.1	8.5	1925
	WRSC	350	650	390	1.2	0.96	4.95	6.8	7.08	2210

5.2. Effect of number of layers of steel meshes of the plastering layers.

Generally, the units with two layers provided better cracking performance than one layer of steel meshes compared with the control units. For Group (GM) it is clear that; the same first cracking load of noticed units with single layers while the ratio was increased for the two layers of steel mesh by 25% for (GND/GMO). The serviceability load, ductility index and energy absorption showed change with the number of layers of reinforced mesh. This illustrates the effect of the stiffness of the columns. The results show that the column specimen (GMD) provided higher ultimate load compared to column specimens GMO. Comparing specimens (GMS) and (GMD) with (GMO) show that the ultimate loads were higher by 33% and 44 %, respectively.

The ratios of the energy absorption of the specimens reinforced with one layer of welded steel mesh (GMS) and the specimens reinforced with two layers (GMD) compared to the control specimens (GMO) were 50% and 65%, respectively. The ratio of the serviceability load of the specimens reinforced with one layer of welded steel mesh (GMS) and the specimens reinforced with two layers (GMD) compared to the control specimens (GMO) were 33% and 45%, respectively.

The ratio of the ductility index of the specimens reinforced with one layer of welded steel mesh (GMS) and the specimens reinforced with two layers (GMD) compared to the control specimens (GMO) were 124% and 139%, respectively. These observations were noticed for the group (WMO). The same first cracking load was noticed for the units reinforced with single layers while the ratio was increased for the two layers of steel meshes by 33% for (WMD/WMO). The results show that the column specimen (WMD) achieved higher ultimate load compared to column specimens WMO. Comparing the specimens (WMS) and (WMD) with (GMO) show that the same ultimate loads were noticed for the specimen WMS while it was higher by 8% for the specimens WMD.

The ratios of the energy absorption of the specimens reinforced with one layer of welded steel mesh (WMS) and the specimens reinforced with two layers (WMD) compared to the control specimens (WMO) were 3% and 6.5%, respectively. The ratio of the serviceability load of the specimens reinforced with one layer of welded steel mesh (WMS) and the specimens reinforced with two layers (WMD) compared to the control specimens (WMO) were 75% and 85%,

respectively. The ratio of the ductility index of the specimens reinforced with one layer of welded steel mesh (WMS) and the specimens reinforced with two layers (WMD) compared to the control specimens (WMO) were -4% and 1.5%, respectively

5.3. Effect of reinforced the core materials

Using core materials to fill the columns was studied. The using of core materials affect on the stiffness, first cracking load, serviceability load, energy absorption, and ultimate load. For example; for specimens (GRO) it is clear that; there is no effect for the core materials for the first cracking load for specimen (GRO) with core material. While an achievement was noticed for serviceability load, energy absorption, and ultimate compared with the control specimen (GMO). The ultimate loads, serviceability load, ductility index and energy absorption were higher by 11%, 11%, 7%, and 42 %, respectively.

5.4. Effect of shear connection.

The effect of using shear connection on the behavior of ferrocemnt columns was observed. The stiffness, first cracking load, serviceability load, energy absorption, and ultimate load were affected by employing shear connection. For test specimens constructed with permanent light weight ferrocement hollow block reinforced with glass fiber; for specimens (GMSC) with shear connection and without core materials; the first cracking load, the serviceability load, the energy absorption, and ultimate load were higher by approximately 25%, 11 %, 42 %, and11 % respectively compared to that of specimen (GMO). When using core materials and the shear connections an increasing (GRSC) was observed for serviceability load, ductility index and the energy absorption by approximately 29%, 91.6 % and 57 % respectively compared to that of specimen (GMSC).

For test specimens constructed with permanent light weight ferrocement hollow block reinforced with steel meshes fiber; for specimens (WRSC) with shear connection and without core materials; the serviceability load, the energy absorption, and ultimate load were higher by approximately 4.7 %, 3.2 % and 8 % respectively compared to that of specimen (WMO). When using core materials and the shear connections an increasing (WRSC) was noticed for the first cracking load, the energy absorption and the ultimate load by approximately 133%, 47% and 8 % respectively compared to that of specimen (WMSC).

Figures 12 and 23 show the load-horizontal displacement curves for the masonry columns under compression load. Also the compressive strains of the masonry columns specimens were emphasized in Figures 24 to 26. The values for the ductility index ($\Delta u/\Delta y$) as a measure of ductility were calculated. The ductility ratio for the columns ranged from 3.08 to 9.69. The increase of the yield load and deflection leads to the reduction of the ductility ratio. Based on the obtained results it is worth mentioning that all columns specimens exhibited first cracking load much lower than the ultimate strength which is a sign of prolonged failure and toughness. It is interesting to note that the ratio of the first cracking loads of the tested specimens to their ultimate loads was approximately nearly 0.3.

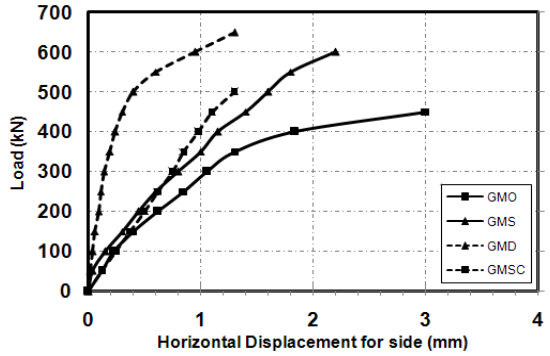

Figure 12: Comparison between experimental results of load – Horizontal displacement for side curves of columns specimens in Group (GM).

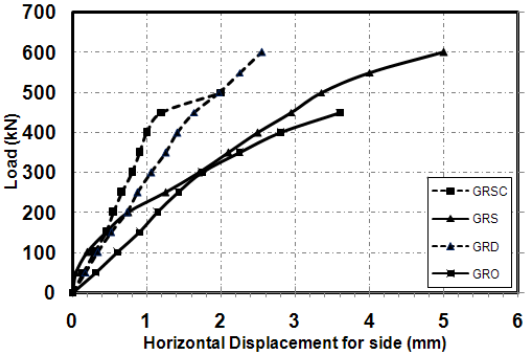

Figure 13: Comparison between experimental results of load – Horizontal displacement for side curves of columns specimens in Group (GR).

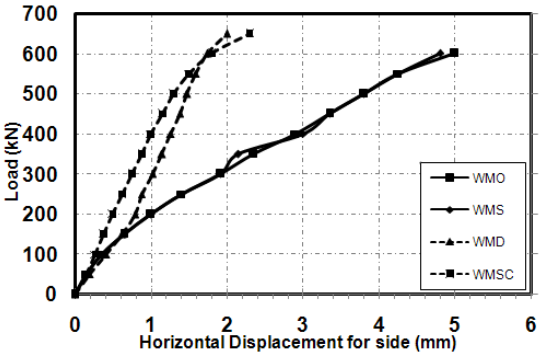

Figure 14: Comparison between experimental results of load – Horizontal displacement for side curves of columns specimens in Group (WM).

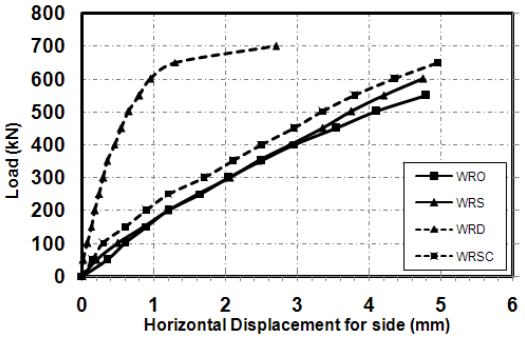

Figure 15: Comparison between experimental results of load – Horizontal displacement for side curves of columns specimens in Group (WR).

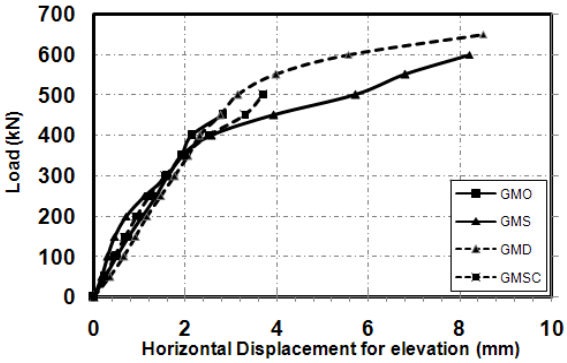

Figure 16: Comparison between experimental results of load – Horizontal displacement for elevation curves of columns specimens in Group (GM).

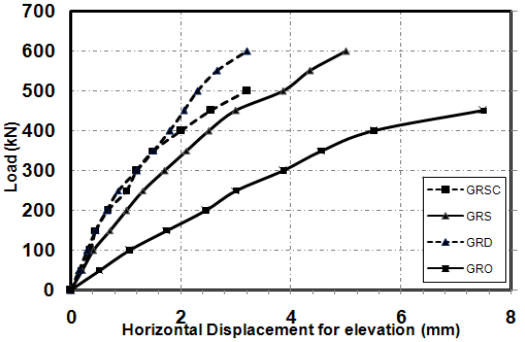

Figure 17: Comparison between experimental results of load – Horizontal displacement for elevation curves of columns specimens in Group (GR).

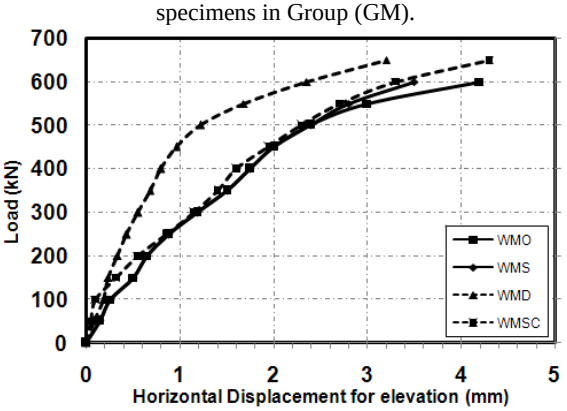

Figure 18: Comparison between experimental results of load – Horizontal displacement for elevation curves of columns specimens in Group (WM).

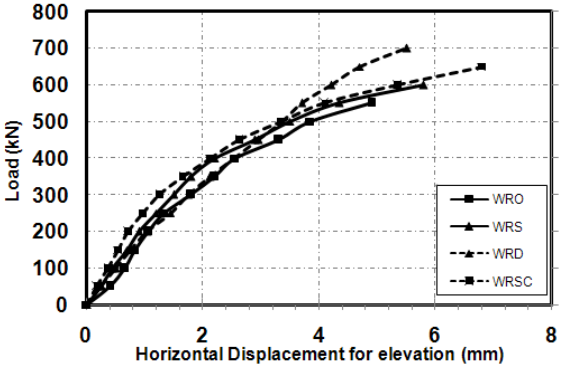

Figure 19: Comparison between experimental results of load – Horizontal displacement for elevation curves of columns specimens in Group (WR).

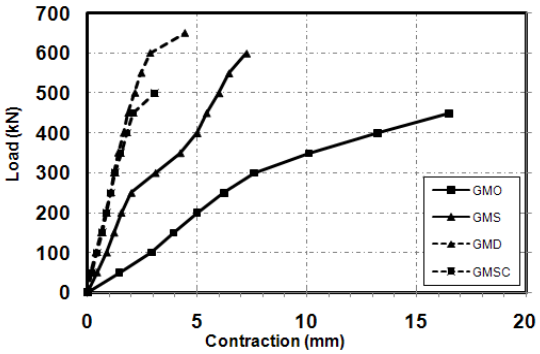

Figure 20: Comparison between experimental results of load – Contraction displacement curves of columns specimens in Group (GM).

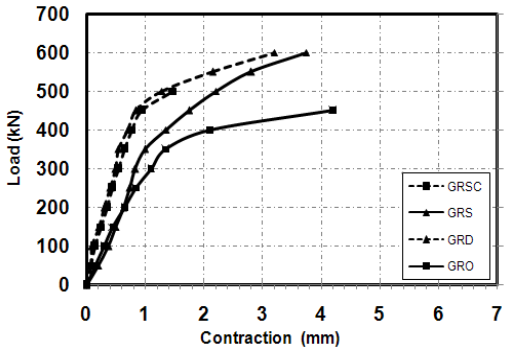

Figure 21: Comparison between experimental results of load – Contraction displacement curves of columns specimens in Group (GR).

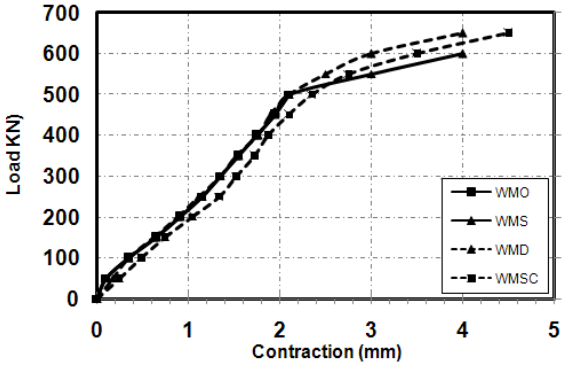

Figure 22: Comparison between experimental results of load – Contraction displacement curves of columns specimens in Group (WM).

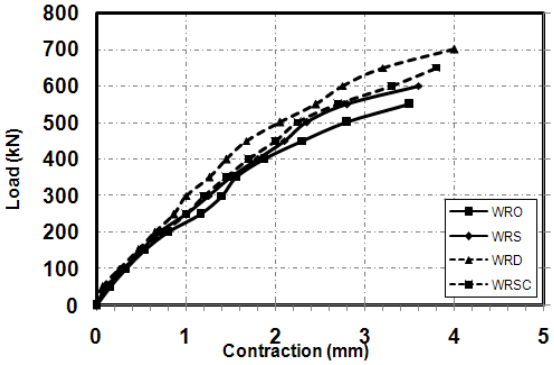

Figure 23: Comparison between experimental results of load – Contraction displacement curves of columns specimens in Group (WR).

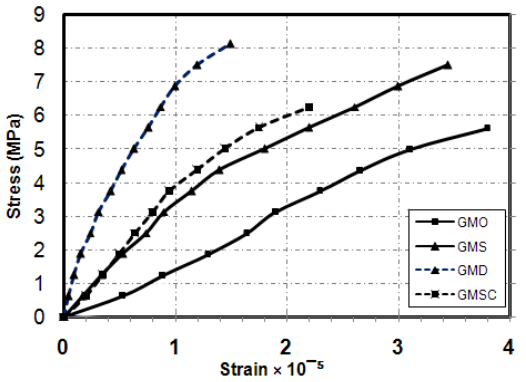

Figure 24: Comparison between experimental results of Strain – Strain curves of columns specimens in Group (GM).

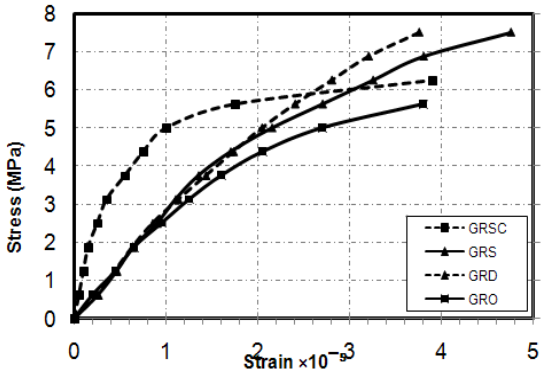

Figure 25: Comparison between experimental results of Strain – Strain curves of columns specimens in Group (GR).

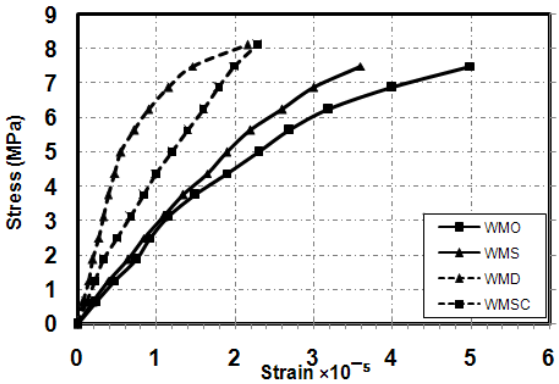

Figure 26: Comparison between experimental results of Strain – Strain curves of columns specimens in Group (WM).

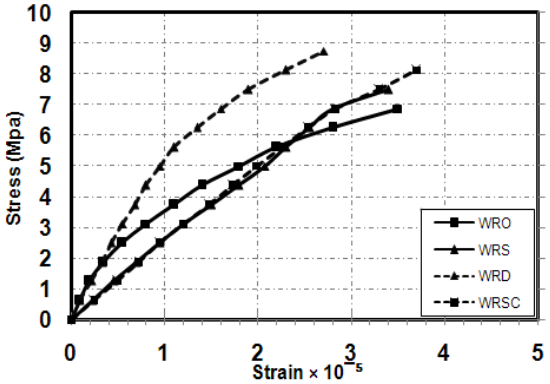

Figure 27: Comparison between experimental results of Strain – Strain curves of columns specimens in Group (WR).

5.5. Mode of failure and behavior of cracking.

Figure 28 illustrates the cracking patterns of the tested columns. The behavior of the tested columns was almost the same. The developed cracks increased as the load increased. On each side new cracks appeared. No spalling of mortar cover was showed at failure this is predominant. The cracking behavior for the columns produced with mortar as core materials were similar to that of the control wall (without core materials).

Figure 28 emphasizes the distribution of cracks on both sides of all columns specimens recorded at different stages of loadings up to failure. These cracks were classified as four types. The crushing of the mortar yielded the cracks of type 1 (when the load capacity reaches 100 to 250 KN; this type of cracking was observed except WRSC was 350 KN).

Some cracks were caused due to the tensile stress crossed the block these types of cracks were occurred when the loads ranged from 400 to 700 KN). At the same time the cracks due to crushing of the bedding mortar were happened. Other crackers were happened between block and mortar due to the rotation of the columns causes the discontact of block and mortar and occurs when the load capacity reaches the ultimate). In all Specimens, a typical failure under axial compression. This behavior is initially explained by the larger deformability of the bed joint mortar with respect to the hollow block. It can be observed that the failure modes of the columns were symmetrical on sides of the specimens. There are no horizontal cracks were observed due to eccentricity of load on the specimens under the flexural test.

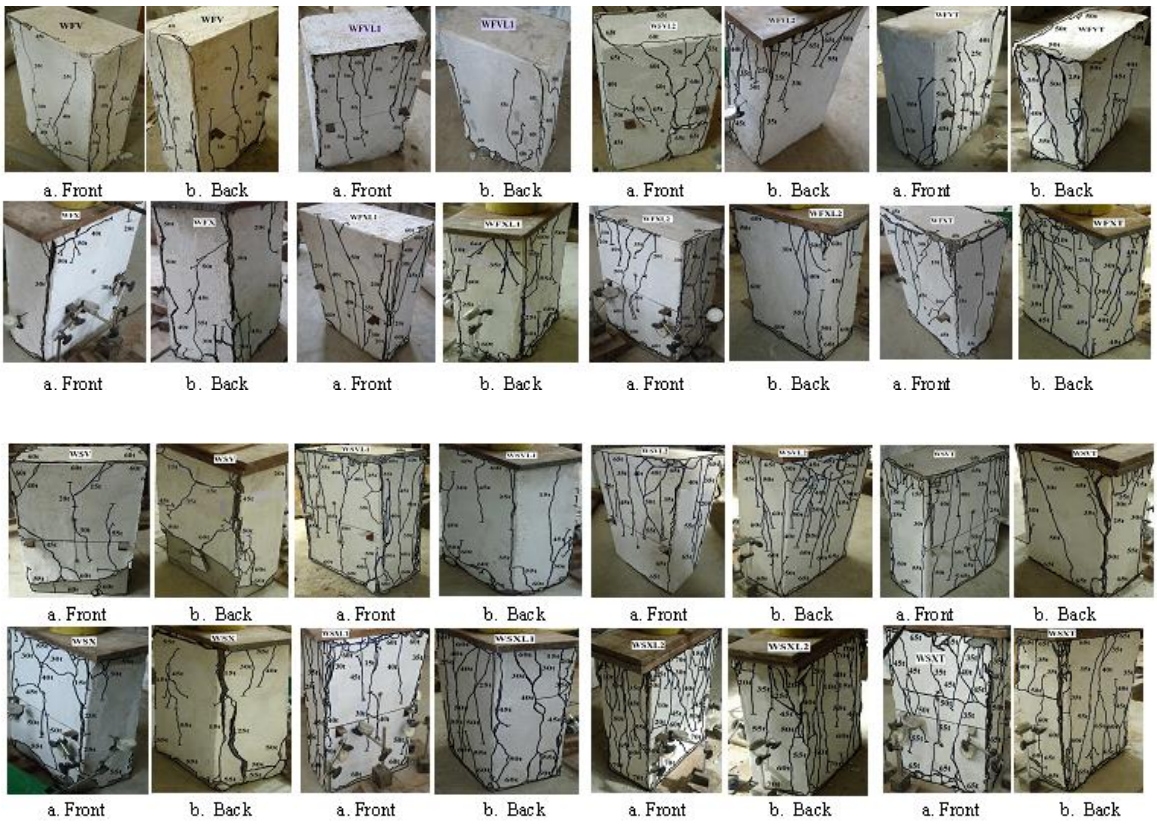

Figure (28) Cracking Pattern of the test Columns.

6. Finite Element Discrimination

A finite element package (ANSYS version 14.5), (ANSYS manual, 1998 and Madenci, E. and Guven, I. (2007)) was used to simulate the behavior of ferrocement lightweight walls. Two types of elements were used; solid 65 and link 8. Figure 29 shows the SOLID65 3-D Reinforced Concrete Solid. Link 8 is defined by two nodes as shown in Figure 30, the cross-sectional area, an initial strain, and the material properties. The element x-axis is oriented along the length of the element from node I toward node J. Figures 31-37 show some theoretical results for the ANSYS program.

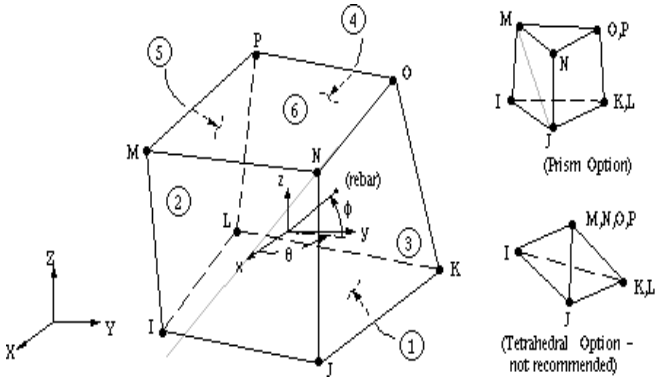

Figure 29: SOLID65 3-D Reinforced Concrete Solid.

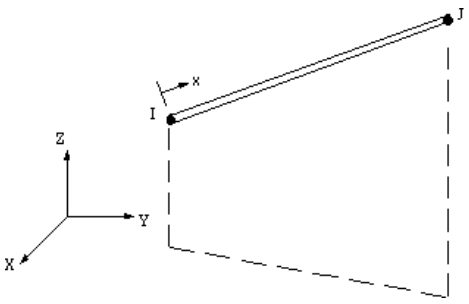

Figure 30: LINK8 3-D Spar.

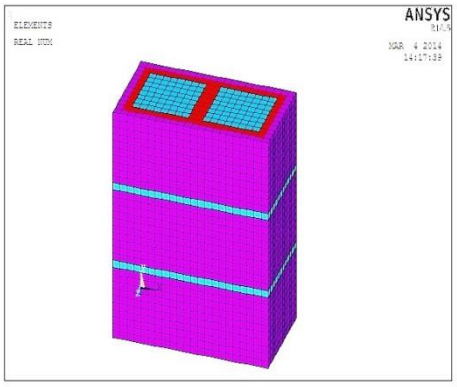

Figure 31: The Configuration of Composite Element Column Model.

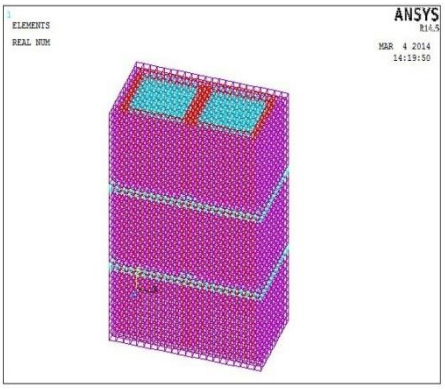

Figure 32: The Configuration of the Steel ElementColumn Model.

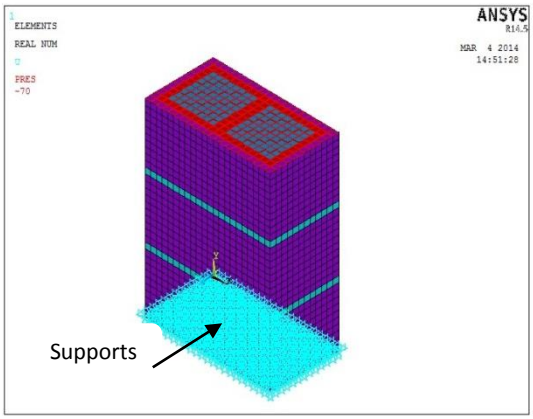

Figure 33: The Configuration of Composite Element column Model under Load and boundary conditions.

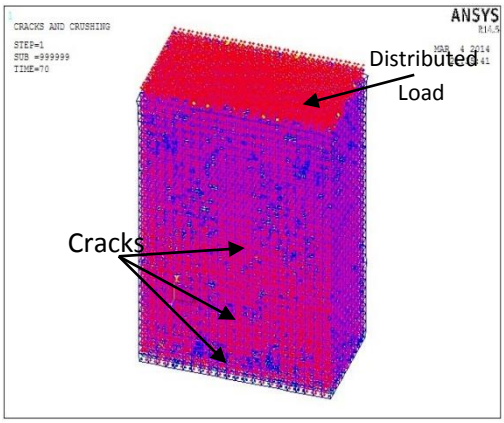

Figure 34: Cracking Pattern at Ultimate Load for Column model.

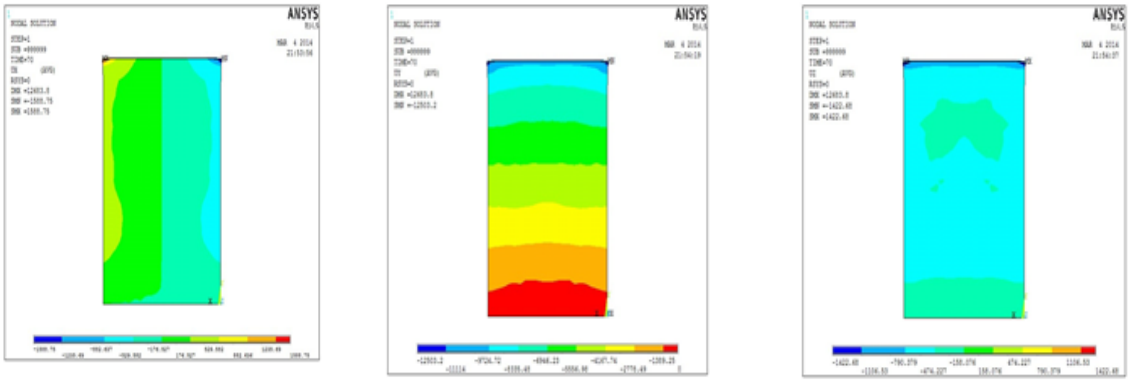

Figure 35: (X, Y&Z) Displacement Resultant Vectors for Column model.

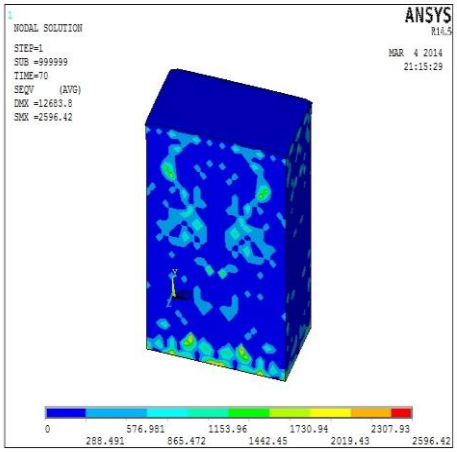

Figure 36: Von-misses Stress Distribution for column Specimen at Ultimate Load.

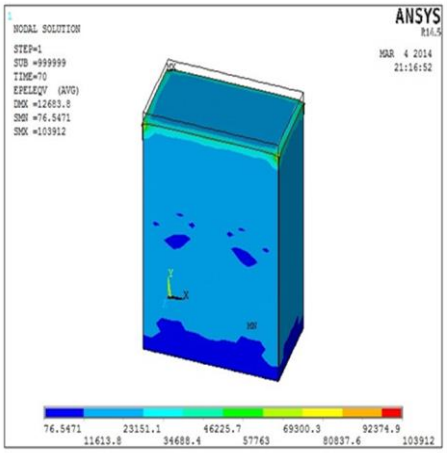

Figure 37: Von-misses Strian Distribution for column Specimen at Ultimate Load.

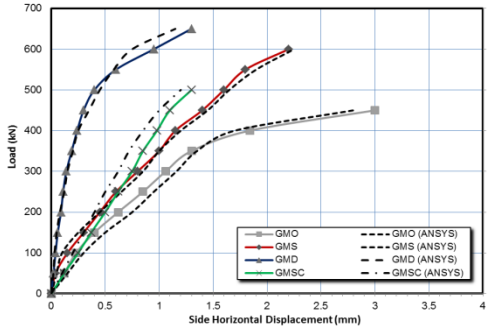

Figure 38: Load- side horizontal displacement Curve for Group (GM).

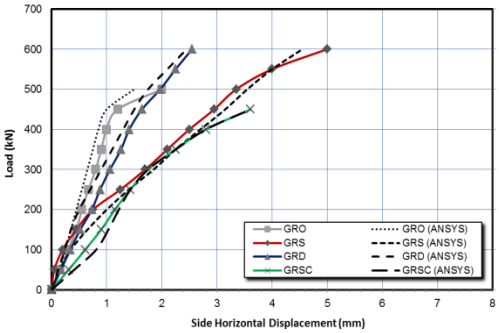

Figure 39: Load- side horizontal displacement Curve for Group (GR).

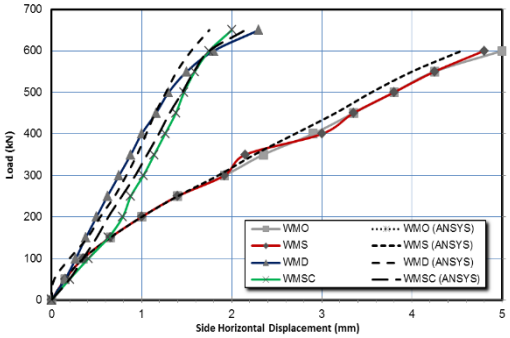

Figure 40: Load- side horizontal displacement Curve for Group (WM).

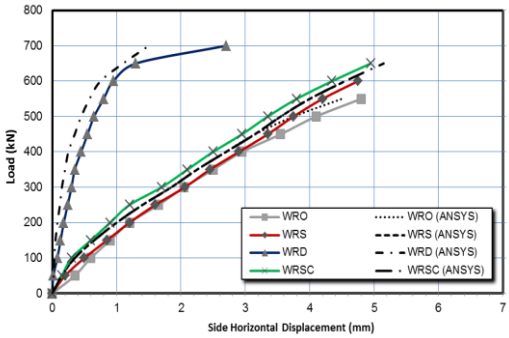

Figure 41: Load- side horizontal displacement Curve for Group (WR).

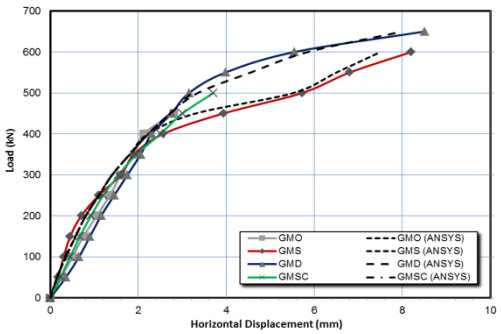

Figure 42: Load- Elevation horizontal displacement Curve for Group (GM).

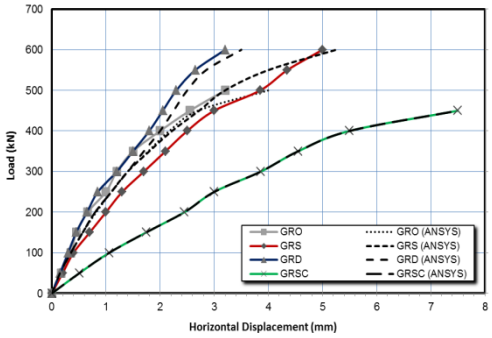

Figure 43: Load- Elevation horizontal displacement Curve for Group (GR).

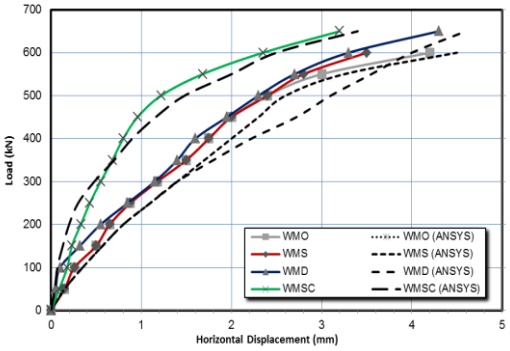

Figure 44: Load- Elevation horizontal displacement Curve for Group (WM).

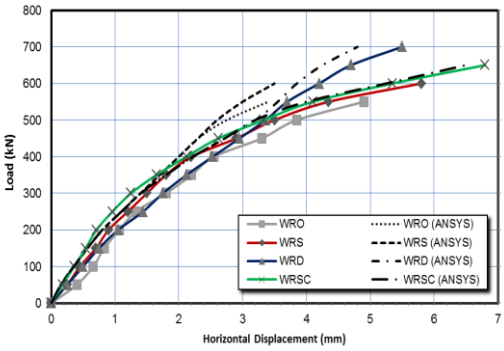

Figure 45: Load- Elevation horizontal displacement Curve for Group (WR).

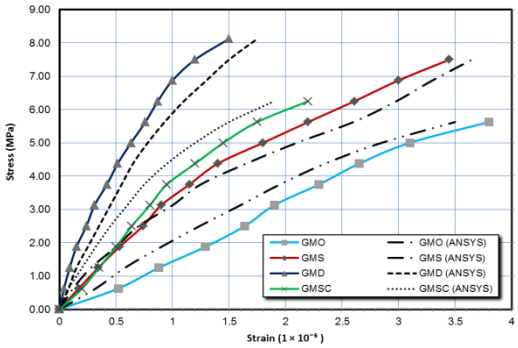

Figure 46: Stress-Strain Curve for Group (GM).

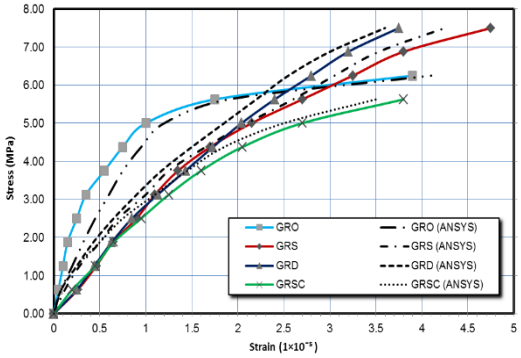

Figure 47: Stress-Strain Curve for Group (GR).

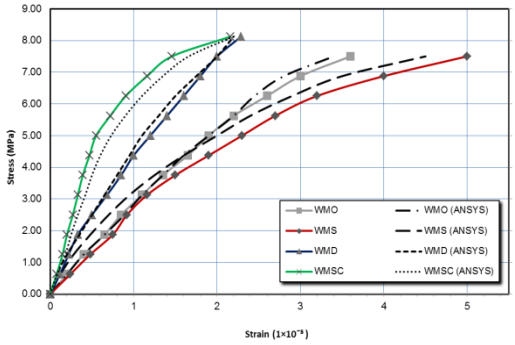

Figure 48: Stress-Strain Curve for Group (WM).

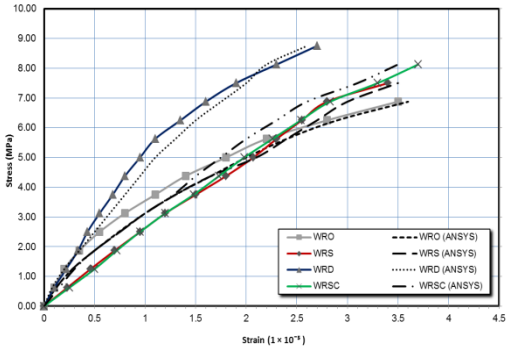

Figure 49: Stress-Strain Curve for Group (WR).

Figures 38-49 show a comparison between the experimental and theoretical results. These results illustrate a good agreement between the theoretical and experimental. Table 5 shows the comparison between theoretical and experimental results for first crack and ultimate loads.

Table 5: Comparison between theoretical and experimental results for first crack and ultimate loads.

Code	First crack load		Ultimate Load	
	$P_{crtheor}$	$P_{crexp}/P_{crtheor}$	P_{utheor}	P_{exp}/P_{utheor}
GMO	190	1.05	455	0.99
GMS	200	1.00	600	1.00
GMD	240	1.04	670	0.97
GMSC	230	1.09	495	1.01
GRO	195	1.03	505	0.99
GRS	210	0.95	570	1.05
GRD	220	0.91	610	0.98
GRSC	160	0.94	480	0.94
WMO	145	1.04	570	1.05
WMS	165	0.91	580	1.03
WMD	190	1.05	630	1.03
WMSC	190	1.05	655	0.99
WRO	150	1.00	535	1.03
WRS	195	1.03	590	1.02
WRD	255	0.98	710	0.99
WRSC	240	1.04	570	0.97
		Ave. = 1.007		**Ave. = 1.003**
		S.D. = .064		**S.D. = 0.029**

7. Conclusions

Due to the experimental results of the present work and within the limitations of the conducted experimental program, the following conclusions could be drawn as follows:

1. Columns specimens constructed using permanent precast lightweight ferrocement hollow block reinforced with galvanized steel meshes achieved ultimate loads reached 33% higher than those reinforced with glass fiber meshes.
2. Employing new innovative technology of producing ferrocement wall units reinforced with longitudinal steel mesh tied with screw bolts in the horizontal direction and filling the cores of blocks with mortar was effective in increasing the load capacity of the developed units by approximately 11% compared with that reinforced with conventional reinforcing materials with great cost savings.
3. Due to higher surface area of using steel meshes resulting in higher bond strength and better controlling of cracking at all stages of loadings. Therefore, sudden loss of rigidity could be avoided as result of the effect of composite action. Consequently higher ultimate load reached 33% and 45% for those reinforced with one and two layers of welded steel meshes respectively.
4. Ultimate, serviceability loads, ductility index and energy absorption were found to be higher by approximately 11%, 11%, 7%, and 42 %, respectively for the columns test specimens with core materials (GRO) compared to those columns without core materials (GMO).
5. Employing shear connections, one layer of welded steel mesh embedded in the mortar between the develop hollow blocks were found to increase the shear capacity of masonry column and better controlling of cracks and their crack widths which are highly significant.

6. First cracking load, serviceability load, ultimate load and energy absorption were found to be higher by approximately 25%, 11 %, 11 %, and 42 % respectively for the column (GMSC) with shear connection and without core materials; compared to that test specimen (GMO).
7. Serviceability load, ductility index and energy absorption properties were found to be higher by approximately 29%, 91.6 % and 57 % respectively for the column (GRSC) with core materials and the shear connections compared with that of specimen (GMSC).
8. First cracking, ultimate loads and energy absorption were reached approximately higher with 133%, 8% and 47 % for the specimens (WRSC) with core materials and the shear connections compared to that specimen (WMSC).

References

1. Wang, S., Naaman A.E. and Li. V.C., (2004) "Bending Response of Hybrid Ferrocement Plates with Meshes and Fibers", *Journal of ferrocement*, **34**(1).
2. Gaba, H., and Singh H., (2008),"The Study of Economy of Ferrocement with Fly Ash as an Admixture", *12th International Conference of International Association for Computer Methods and Advances in Geomechanics* (IACMAG), 1-6.
3. Naaman A. E., (2000) "Ferrocement and Laminated Cementitious Composites". *Ann Arbor, Michigan, USA: Techno Press. Materials and Structures*, **33** (2).
4. Wafa, M.a., and Fukuzawa K., (2010) "Characteristics of Ferrocement Thin Composite Elements Using Various Reinforcement Meshes in Flexure". *Journal of Reinforced Plastics and Composites*, **29**(23), 3530-3539.
5. Eltehawy, E., (2009), "Effect of Using Ferrocement on the Mechanical Properties of Reinforced Concrete Slabs Subjected to Dynamic Loads". *13th International Conference on Aerospace Science and Aviation Technology (ASAT)*, 1-13.
6. Jagannathan, A. (2005) "Flexural and Impact Strength Characteristics of Polymer Mesh Reinforced Ferrocement PANELS", PhD Thesis, Department of Civil Engineering, Pondicherry Engineering College, 605014 Pondicherry.
7. Greepala and Nimityongskul, (2008), "Structural Integrity of Ferrocement Panels Exposed to fire". *Cement and Concrete Composites;* **30** (5), 419-430
8. Sasiekalaa, K. and Malathy R., (2012), "A Review on Mechanical Properties of Ferrocement with Cementitious Materials". *International Journal of Engineering Research and Technology*, **1**(9).
9. ACI Committee 549. (1997), "State-of-the-Art report on ferrocement". *ACI549-R97, in manual of concrete practice. ACI, Detroit*, 26pp.
10. D'Ayala D. "Unreinforced Brick Masonry Construction". University of Bath, United Kingdom.
11. ACI Committee 213R-87 (1999), "Guide for Structural Lightweight Aggregate Concrete". ACI Manual of Concrete Practice.
12. Tawab, A.A., E.H. Fahmy and Y.B. Shaheen, (2012) "Use of Permanent Ferrocement Forms for Concrete Beam Construction". *Materials and Structures*, **45**(9): 1319-1329.
13. Fahmy E. H., Shaheen Y. B. I., Abdelnaby A. M., and AbouZeid M. N.,(March 2014) " Applying the Ferrocement Concept in Construction of Concrete Beams Incorporating Reinforced Mortar Permanent Forms" *International Journal of Concrete Structures and Materials*; **8** (1):83–97.
14. Mustapha, M.L. and Salihuddin, R.S. (2013) "A Review Study on Cold-Formed-Ferrocement Composites" *Australian Journal of Basic and Applied Sciences*, **7**(9): 103-111.

15. Bhalsing S., Shoaib S. and Autade P., (April 2014) "Tensile Strength of Ferrocement with Respect to Specific Surface". *International Journal of Innovative Research in Science, Engineering and Technology*; **3** (4).
16. Grija S., Sivakumar P., Lakshmikandhan K. N., Ravichandran R., Karthikeyan B. (2014)" Novel Ferrocement Light Weight Wall Panels", *International Journal of Applied Engineering Research* , **9** (18): 4645-4657 http://www.ripublication.com
17. Fahmy E. H., AbouZeid M. N., Shaheen Y. B., and Gaafar H., (2005), "Behavior of Ferrocement Panel under Axial and Flexural Loadings". *Journal of the American Concrete Institute*, **79** (4), 313-321.
18. Al-Rifaie W.N. and Jomaah M. M. (22-23 Dec. 2010) "Structural Behavior of Ferrocement System for Roofing" *First Engineering Scientific Conference*-College of Engineering –University of Diyala,: 237-248
19. Shaheen Y. B.I., Etman Z. A., and Ramadan A. G. (2014), "Feasibility of Producing Ferrocement Lightweight Hollow Blocks", *AICSGE8 - The eighth Alexandria international conference on Structural and Geotechnical Engineering*, Department of Structural Engineering, Faculty of Engineering, Alexandria University, Egypt.
20. Egyptian Standards Specification, E.S.S, 4756-11, (2007), (physical and mechanical properties examination of cement, part 1), Cairo.
21. ASTM C494/C 494M, (2001), "Standard Specification for Chemical Admixtures for Concrete", Annual Book of ASTM Standards **04**, 02, p.9.
22. BS EN 934-2:2009+AR2012, (30 June 2009) "Admixtures for Concrete, Mortar and Grout Concrete admixtures". Definitions, requirements, conformity, marking and labeling, p. 28.
23. ASTM C90 – 11, (2011), "Standard Specification for Load Bearing Concrete Masonry Units". Standard, West Conshohocken, Pennsylvania: ASTM International.
24. ASTM C129 – 06, (2007), Standard Specification for No-Load Bearing Concrete Masonry Units. Standard, West Conshohocken, Pennsylvania: ASTM International.
25. International Building Code. International Code Council, 2012.
26. E.S.S 2005/42 *Standards for Solid Bricks and Hollow Blocks, Standard*, Cairo, Egypt: Egyptian Organization for Standardization and Quality, 2005.
27. ASTM C270-07, *Standard Specification for Mortar for Unit Masonry West Conshohocken, Pennsylvania*: ASTM International, 14 p, 2007.
28. Egyptian Code for Concrete structures, Cairo, 2007.
29. ANSYS, ANSYS Manual Set, 1998, ANSYS Inc., South point, 275 Technology Drive, Canonsburg, PA 15317, USA. ANSYS Manual, Version (14.5).
30. Madenci, E. and Guven, I. (2007), "The Finite Element Method and Applications in Engineering Using ANSYS®", , 686 p. ISBN 978-0-387-28290-9, http://www.springer.com/978-0-387-28289-3